Published May 1, 1985

Nonlinear Cable Properties of the Giant Axon of the Cockroach *Periplaneta americana*

IDAN SEGEV and ITZCHAK PARNAS

From the Neurobiology Department, Institute of Life Sciences, The Hebrew University, Jerusalem, Israel

ABSTRACT The steady state nonlinear properties of the giant axon membrane of the cockroach *Periplaneta americana* were studied by means of intracellular electrodes. The resistivity of this membrane markedly decreases in response to small subthreshold depolarizations. The specific slope resistance is reduced by twofold at 5 mV depolarization and by a factor of 14 at 20 mV depolarization. As a result, the spatial decay, $V(X)$, of depolarizing potentials is enhanced when compared with the passive (exponential) decay. This enhancement is maximal at a distance of 1–1.5 mm from a point of subthreshold (0–20 mV) depolarizing perturbation. At that distance, the difference between the actual potential and the potential expected in the passive axon is ~30%. The effects of membrane rectification on $V(X)$ were analyzed quantitatively with a novel derivation based on Cole's theorem, which enables one to calculate $V(X)$ directly from the input current-voltage (I_0-V) relation of a long axon. It is shown that when the experimental I_0-V curve is replotted as $(I_0R_{in})^{-1}$ against V (where R_{in} is the input resistance at the resting potential), the integral between any two potentials ($V_1 > V_2$) on this curve is the distance, in units of the resting space constant, over which V_1 attenuates to V_2. Excellent agreement was found between the experimental $V(X)$ and the predicted value based solely on the input I_0-V relation. The results demonstrate that the rectifying properties of the giant axon membrane must be taken into account when the electrotonic spread of even small subthreshold potentials is studied, and that, in the steady state, this behavior can be extracted from measurements at a single point. The effect of rectification on synaptic efficacy is also discussed.

INTRODUCTION

Linear cable theory has proven to be very fruitful for studying the role of subthreshold potentials in neuronal information processing, yielding new insights concerning the importance of cell geometry as well as the role of specific membrane properties (Hodgkin and Rushton, 1946; see also reviews by Taylor, 1963; Cole, 1968; Jack et al., 1975; Redman, 1976; Rall, 1977; Turner and Schwartzkroin, 1984). However, in order to apply linear cable theory to nerve

Address reprint requests to Dr. Idan Segev, Mathematical Research Branch, National Institute of Arthritis, Metabolism and Digestive Diseases, NIH, Bldg. 31, Rm. 4B50, 9000 Rockville Pike, Bethesda, MD 20205.

J. GEN. PHYSIOL. © The Rockefeller University Press · 0022-1295/85/05/0729/13 $1.00 729
Volume 85 May 1985 729–741

cells, it is usually assumed that the neuron membrane is passive at subthreshold potentials (i.e., that membrane properties are voltage-independent). Indeed, the conventional concept of the space constant (λ), which was used for describing the spatial parameters and behavior of potentials in neurons (such as their electrical length and the decay of potentials with distance), is meaningful only for passive membranes.

The linear model, of course, is only an approximation (Hodgkin and Huxley, 1952), and, in reality, the membrane properties of most neurons change as a function of potential (i.e., the membrane rectifies), even near the resting potential (for a review on this matter, see Grundfest, 1967). Perturbations in membrane potential produced by synapses or by current injection from microelectrodes decay as they spread along nerve cell processes and thus affect the voltage-sensitive resistance of each successive patch of membrane differently. In such situations, the attenuation of potential is difficult to predict.

The first analytical approach to the question of membrane rectification was devised by Cole and Curtis in 1941 (see also Cole, 1961). They described an elegant method for calculating how ionic current through a membrane, $i_m(V)$, varies with membrane potential, V, using the experimental input current-voltage relation (I_0-V) of an infinite axon. If r_i is the axoplasmic resistance per unit length and the extracellular resistance is assumed to be negligible, this method (known as Cole's theorem) yields

$$i_m(V) = \frac{r_i}{4} I_0 \frac{dI_0}{dV}, \tag{1}$$

where i_m is membrane current per unit length, I_0 is the applied steady current, and V is the potential displacement at the point where the current is applied, (i.e., at $x = 0$; see Fig. 1). This theory was further extended and applied to study threshold phenomena in electrically short muscles (Adrian et al., 1972). Cole's theorem was also used by Jack et al. (1975) to study the spatial distribution of steady state potentials in nonlinear cylindrical cables. In doing so, $i_m(V)$ had to be approximated by a polynomial (see also Kootsey, 1977; Anderson and Arthurus, 1978; Arthurus and Arthurus, 1983). Other investigators used numerical approximations to $i_m(V)$ together with computational approaches to tackle this question (Noble, 1962; Arispe and Moore, 1979; Joyner and Westerfield, 1982).

Although the intrinsic and sometimes marked nonlinearities of neuron membranes at subthreshold potentials are well known, the mathematical complications and the need for approximations have limited quantitative studies of the spatial distribution of potentials in excitable cells. The present work illustrates how the effect of membrane rectification on the spatial behavior of steady potentials in long axons can be extracted simply from measurements of input resistance, with no need for any approximations. This approach was used in the case of the giant axons of the cockroach *Periplaneta americana*, where membrane rectification at depolarizing subthreshold potentials is shown to be significant. It is hoped that the approach presented here will simplify quantitative analysis of the role of membrane rectification in the integrative properties of neurons.

METHODS

Preparation

Adult male cockroaches (*Periplaneta americana*) were used. The whole ventral nerve cord was isolated as previously described (Spira et al., 1969). The cord was pinned ventral side up in a Sylgard chamber for easier access to the ventral giant axons. The bathing solution was composed of 214 mM NaCl, 3.1 mM KCl, 9 mM $CaCl_2$, and 1 mM Tris (Kerkut et al., 1969). The pH was adjusted to 7.4.

Recording and Stimulation

Intracellular recording and current injection were done with glass microelectrodes filled with 3 M K-acetate or 3 M KCl (10–15 M resistance) using conventional electrophysiological techniques. Intracellular recordings were made between the A_4 and A_5 ganglia. This region is relatively long (4–6 mm) and the giant axons have a constant diameter of ~40 μm (Yarom, 1978). The T_2–T_3 and A_5–A_6 connectives were stimulated extracellularly with AgCl hook electrodes. The criteria of Spira et al. (1976) were used in deciding whether the microelectrodes had penetrated an abdominal giant axon (Fig. 1).

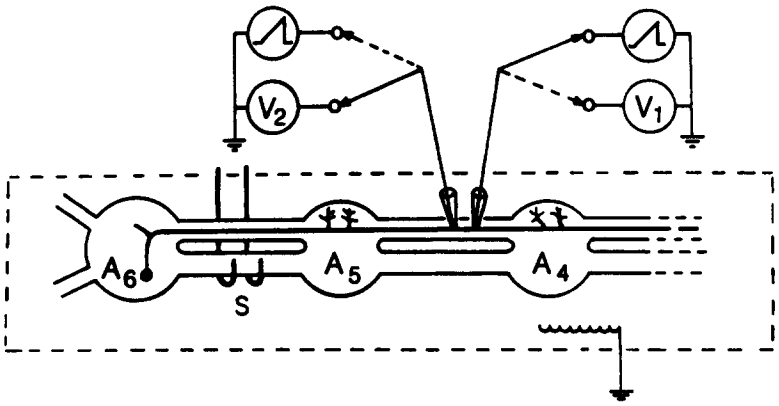

FIGURE 1. Schematic drawing of the experimental procedure. Current and voltage electrodes were inserted into a giant axon between the A_4 and A_5 ganglia. Each of these electrodes could either record potential (V_1 and V_2) or inject current. One extracellular hook electrode was placed between the A_4 and A_6 ganglia (S) and another between the T_2 and T_3 ganglia (not shown). These electrodes were used to initiate antidromic or orthodromic action potentials in the giant axon.

In each experiment, one intracellular electrode was used for passing current and remained at a fixed ($x = 0$) point, while another electrode recorded voltage at different distances from the first. In order to minimize possible effects of axon damage caused by the microelectrode penetrations, the voltage electrode was initially inserted at the maximum distance from the current electrode, and then moved successively closer (i.e., from *d* to *a* in Fig. 3*C*). The last measure (at *a* in Fig. 3*C*) was done with the two electrodes separated by <40 μm. At each distance, the resting potential and the action potential were recorded first. Then a slow current ramp ($I_0/t < 10$ μA/s) was injected through the current electrode and the voltage displacement was measured in the second one. The applied current was input to the horizontal amplifier of a digital oscilloscope, while the

voltage was input to the vertical amplifier (Cole and Curtis, 1941). At each interelectrode distance, a complete current-voltage (I_0-V) curve was obtained. The spatial attenuation of voltage along the giant axon was then calculated from the I_0-V curves, and the results were compared with the theoretical predictions. Axons were accepted for analysis only when the resting potential and the action potential were the same in both electrodes at all recording points (Fig. 2*B*).

THEORY

Extracting the Steady Attenuation of Potentials, V(X), from the Input I_0-V Relation

From the linear cable theory, it is known that the input resistance of an infinite cable is

$$R_{in} = \frac{1}{2}[r_m(0)r_i]^{1/2}, \tag{2}$$

where $r_m(0)$ is the membrane resistance times unit length at $V = 0$ (Hodgkin and Rushton, 1946). Let us define $U = I_0 \cdot R_{in}$, where I_0 is the applied current and R_{in} is the slope resistance of the input current-voltage relation at the resting potential ($V = 0$). Taken together with Eq. 2, Cole's theorem (Eq. 1) becomes

$$i_m(V) = \frac{1}{r_m(0)} U \frac{dU}{dV}. \tag{3}$$

Note also that $(dU/dV)_{V=0} = 1$; $U(0) = 0$.

In a cable, the steady state membrane current is proportional to the second derivative of the potential with distance:

$$i_m(V) = \frac{1}{r_i} \frac{d^2V}{dx^2}. \tag{4}$$

Following the derivations of Adrian et al. (1972) and of Jack et al. (1975), Eq. 4 is multiplied on both sides by $2\frac{dV}{dx}$ to give

$$2\frac{dV}{dx} i_m(V) = \frac{1}{r_i} \frac{d}{dx}\left[\left(\frac{dV}{dx}\right)^2\right]. \tag{5}$$

Integrating both sides between infinity and x,

$$\pm\left[2r_i \int_{V_\infty}^{V_x} i_m(V)dV\right]^{1/2} = \left(\frac{dV}{dx}\right)_x, \tag{6}$$

noting that $\left(\frac{dV}{dx}\right)_\infty = 0$.

If we take only positive values of x, then the negative sign in Eq. 6 is required. Separating variables and integrating between 0 and x,

$$\int_{V_0}^{V_x} \frac{dV}{\left[2r_i \int_{V_\infty}^{V} i_m(V)dV\right]^{1/2}} = -x, \tag{7}$$

which relates the spatial attenuation of potential to the membrane current-voltage relation.

If $i_m(V)$ is represented by a polynomial, this equation can be solved analytically (Adrian et al., 1972; Jack et al., 1975, pp. 394–397). However, in an experiment where only the input I_0-V relation is known directly, $i_m(V)$ need not be calculated (and then approximated) in order to obtain the spatial spread of steady potentials. Substituting $i_m(V)$ from Eq. 3 into Eq. 7 gives

$$\int_{V_0}^{V_x} \frac{dV}{\left[2\frac{r_i}{r_m(0)}\int_{V_\infty}^{V} UdU\right]^{1/2}} = -x. \tag{8}$$

Since $V_\infty = 0$ and $U(0) = 0$, we obtain

$$\int_{V_0}^{V_x} \frac{dV}{\left[\frac{r_i}{r_m(0)}U^2\right]^{1/2}} = -x, \tag{9}$$

and finally we get

$$\int_{V_0}^{V_X} \frac{dV}{I_0 R_{in}} = -X, \tag{10}$$

where $X = x/\lambda_0$ and $\lambda_0 = [r_m(0)/r_i]^{1/2}$ is the space constant at the resting potential (i.e., the "resting space constant"; see the Discussion).

Eq. 10 suggests a simple graphical method for extracting $V(X)$ directly from the experimental nonlinear input current-voltage relation. If one plots $(I_0R_{in})^{-1}$ against V, the area (in dimensionless units) that lies below this curve between two potentials, $V_1 > V_2$, is the distance (in units of λ_0) over which V_1 attenuates to V_2. This is shown schematically in Fig. 3, *A* and *B*.

RESULTS

A typical case of rectification in the giant axon membrane is shown in Fig. 2*A*. The continuous line shows the input current-voltage relation of that axon. In this case, the distance between the current and the voltage electrode is 40 μm (see Methods). This membrane exhibits marked nonlinearity even with a small depolarization (Table I). At hyperpolarizing potentials, the membrane is essentially linear. The specific I_m-V relation is also shown in the same figure (dotted line). This line was obtained from Cole's theorem (Eq. 1), assuming an axon diameter of 40 μm and a specific axoplasmic resistance of 132 Ω·cm (Yarom, 1978). In order to facilitate comparison between the shapes of the two curves, the highest point on the right and the lowest point on the left in the I_m-V curve (dotted line) were superimposed on the corresponding points in the I_0-V curve (continuous line). As described in the Methods section, the I_0-V measurement in each experiment was preceded by recording the action potential in both the current and the voltage electrodes (Fig. 2*B*). The simultaneous appearance of the action potential peak in both electrodes shows that there was very little distance between them.

As predicted by Jack et al. (1975), the I_0-V curve in Fig. 2*A* displays less outward rectification than does the corresponding I_m-V curve. This is a result of the cable properties of axons, which tend to linearize the rectifying properties of their membranes. These properties were studied in five giant axons by measuring their membrane current-voltage curves. The specific slope resistances of these axons (i.e., the slopes of their I_m-V curve) at different depolarizing potentials were calculated and the results are given in Table I. As can be seen, the slope resistance drops by a factor of 2 at 5 mV depolarization, and decreases by a factor of 14 at 20 mV depolarization. These values are comparable to those found in the squid giant axon (Cole, 1968; Arispe and Moore, 1979) and in other excitable tissues (cf. Kandel and Tauc, 1966).

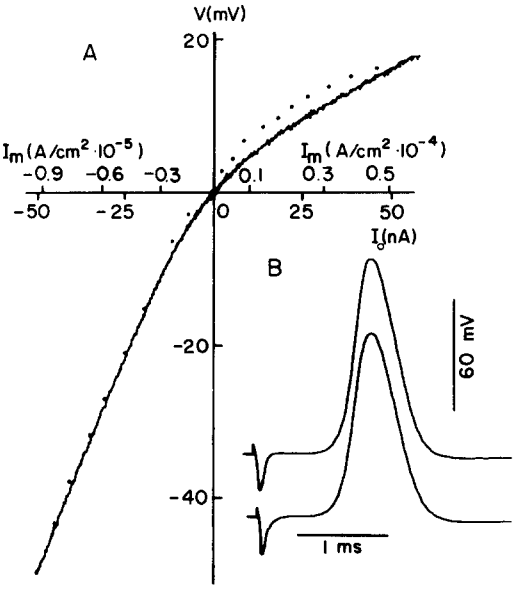

FIGURE 2. (*A*) I_0-V relation (continuous curve) and I_m-V relation (dotted curve) in a giant axon. The lower scale of the abscissa is for the injected (I_0) current; the upper one is for the specific (I_m) current. Note the difference in scales for the specific current in the hyperpolarizing and depolarizing directions. The electrode separation is 40 μm. (*B*) Action potential recorded by the two electrodes, which were later used in producing the I_0-V curve of *A*.

The effect of rectification on the spatial decay of steady potentials was also analyzed (see Methods). An example is shown in Fig. 3*C*. The continuous line *a* shows the input current-voltage relation recorded with negligible separation between the current and voltage electrodes. The continuous lines of curves *b*, *c*, and *d* give the relation between I_0 and the voltage recorded at distances of 0.6, 0.9, and 1.15 mm, respectively, from the current source. As expected from theoretical considerations (Segev, I., manuscript in preparation), the apparent nonlinearity in the depolarizing direction seems to increase as the distance between the electrodes increases, while it remains linear for all distances in the hyperpolarizing direction (see also Noble, 1962).

Eq. 10 predicts $V(X)$ from the experimental I_0-V relation for any value of I_0. To compare these experimental results with the theoretical prediction of Eq. 10, two scaling steps are required: (*a*) the actual distance must be expressed in units of the "resting space constant," and (*b*) the injected current must be multiplied by the corresponding (resting) input resistance (see Theory and the Discussion). Since the axon membrane is linear in the hyperpolarizing direction, the potential produced by a hyperpolarizing current will decay exponentially with distance. Therefore, for a given hyperpolarizing input current, normalized distances can be calculated directly from the ratio of the voltage recorded at point *a* to the corresponding voltages at locations *b*, *c*, and *d*. In the case of Fig. 3*C*, the electrical distances ($X = x/\lambda_0$) between point *a* and points *b*, *c*, and *d* were found to be 0.246, 0.379, and 0.471, respectively (which implies that $\lambda_0 \simeq 2.4$ mm). The injected current was multiplied by the slope of curve *a* at the resting potential, and the method described in Fig. 3, *A* and *B*, was then applied.

TABLE I

Specific Slope Resistance as a Function of Depolarization in Five Giant Axons

	Specific slope resistance					
Potential	Axon 1	Axon 2	Axon 3	Axon 4	Axon 5	Average (± SD)
mV			$\Omega \cdot cm^2$			
0 (Rest)	2,340	3,300	1,500	3,500	3,500	2,830 (884)
+5	1,100	1,640	900	2,000	2,100	1,550 (533)
+10	740	1,000	550	1,040	1,100	890 (233)
+15	275	330	410	700	800	500 (233)
+20	80	200	150	100	450	200 (150)

The decay with distance of four initial potentials was calculated using the I_0-V relation of the *a*, *b*, *c*, and *d* distances and is shown by the filled circles in Fig. 3*C*. The four initial potentials chosen (20, 17.5, 15, and 12.5 mV) are marked by the filled circles on curve *a*; their predicted attenuation is shown by the corresponding filled circles in curves *b*, *c*, and *d*. As can be seen, the attenuation that was found experimentally at these distances can be extracted very accurately when applying the method described above to curve *a* alone.

The significance of this result is that in a long, uniform, nonlinear cable, the spatial behavior of steady state potentials can be deduced from measurements at a single point. Using the method described above on curve *a* in Fig. 3*C*, a family of curves was obtained describing $V(X)$ for initial depolarizing voltage steps of 5, 10, and 20 mV (Fig. 4*A*). As expected, it can be seen that rectification enhances the decay of potential in comparison with the exponential decay expected in a passive cable (dashed line). In the latter case, any initial potential should decay to half its initial value at a distance of $X = 0.693$. In nonlinear cables, the decay depends on the value of the initial potential, and for the rectification observed in the giant axon, it increases with depolarization (Jack et al., 1975). For example, in the axon of Fig. 4, the half-decay distance is decreased from 0.693 to 0.626, 0.546, and 0.395 for initial potentials of 5, 10, and 20 mV, respectively.

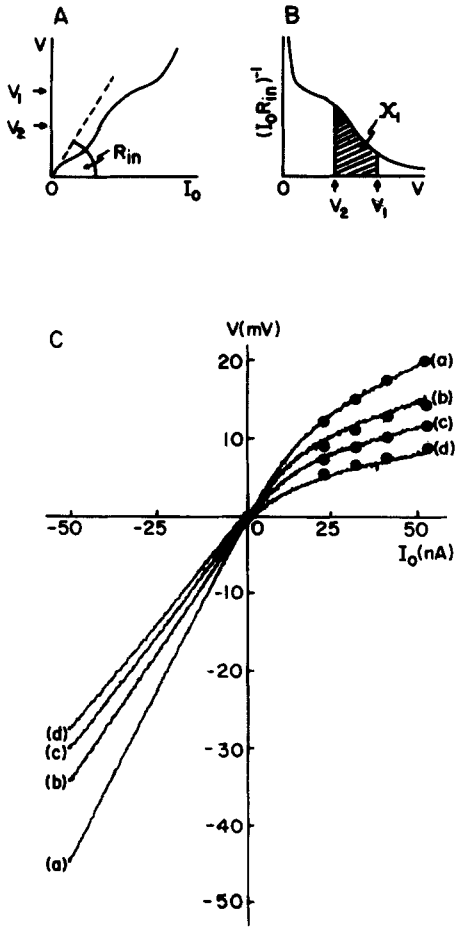

FIGURE 3. Calculation of the spatial attenuation of steady state potentials in an arbitrary nonlinear infinite cable and in the giant axon of the cockroach. (*A* and *B*) Schematic representation of the method for calculating the steady state attenuation of potential with distance in an infinite cable, derived from the current-voltage relation at one point. The current-voltage curve is given by the continuous line in *A*. R_{in} is the input resistance at the resting potential, I_0 is the applied current, and V is the potential measured at the point where the current is applied. From this curve, the graph of $(I_0R_{in})^{-1}$ is plotted against V in *B*. The dimensionless integral, X_1, between two arbitrary voltages, $V_1 > V_2$, is the distance in units of the resting space constant over which V_1 attenuates to V_2. (*C*) Spatial decay of steady state potentials in the cockroach giant axon. The experimental input current-voltage relation of the giant axon is given by the continuous line *a*; the continuous lines *b*, *c*, and *d* give the relation between the applied current and the voltage when measured at distances of $x = 0.6$, 0.9, and 1.15 mm, respectively, from the current source ($x = 0$). The filled circles show the spatial decay of four initial potentials ($V_0 = 20$, 17.5, 15, and 12.5 mV), which is predicted from the experimental curve *a* using the method described in *A* and *B* (see text).

Published May 1, 1985

The spatial effect of the nonlinearity in the giant axon membrane can be appreciated if one plots the difference between the potential in the linear case and the potential in the giant axon, as a function of distance (Fig. 4*B*). For any value of V_0 (indicated in each curve), there is a distance at which this deviation

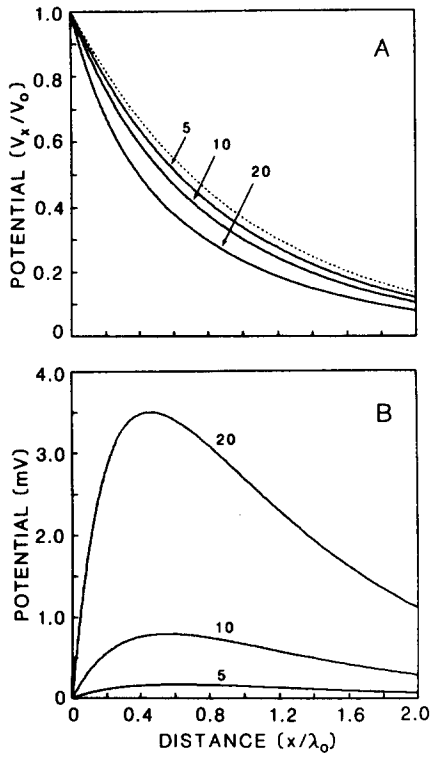

FIGURE 4. Effect of nonlinearity on the spatial decay of steady state potentials in the giant axon. (*A*) The spatial attenuation, normalized in terms of the initial potential, V_0, for three initial potential values (given in millivolts on the continuous curves). The dashed line shows the exponential decay expected in a linear membrane. (*B*) The difference between nonlinear decay, shown in the solid curves in *A*, and linear decay (dotted curve in *A*), as a function of distance from the point of origin. The values (in millivolts) of the initial potentials are marked in each curve. Note that the potentials were not normalized and the ordinate units are in millivolts.

from linearity is maximal. For the axon analyzed here, and for an initial depolarization of 5, 10, and 20 mV, this distance is 0.4–0.6 λ_0. It is of interest that this distance is approximately the distance between ganglia in the adult cockroach. Thus, with measurements made at this distance, it is particularly important that membrane nonlinearity be taken into account when the degree of spatial decay of steady state potentials through the ganglion is calculated.

DISCUSSION

The results show that membrane rectification has a significant effect on the cable properties of the cockroach giant axon even at depolarizations of a few millivolts. The derivation given in Eq. 10 provides a simple method of extracting the steady state nonlinear cable properties of long fibers from measurements at a single point (Fig. 3, *A* and *B*). This approach complements Cole's theorem, which enables one to study the membrane characteristics of such fibers from input current-voltage relations.

In using Cole's theorem, it was found that in the giant axon, the decrease in the specific slope resistance with depolarization is roughly 14-fold in the subthreshold range of 0–20 mV. This degree of rectification seems to be typical of many preparations (see, for example, Cole, 1968; Arispe and Moore, 1979; Tauc and Kandel, 1966; Trifonov et al., 1974). Given an average diameter of 40 μm, the specific slope resistance of the giant axon drops from 2,800 $\Omega \cdot cm^2$ at resting potential to ~200 $\Omega \cdot cm^2$ at 20 mV depolarization (Table I). As a consequence, the response caused by a small steady state perturbation in voltage about the resting potential will be 14-fold larger than the one about 20 mV depolarization (Jack et al., 1975, p. 227). This suggests that rectification could serve as a postsynaptic mechanism to dynamically modulate the response to a given input (see below).

Using the derivation of Eq. 10, it can be shown that for any nonlinear cable properties and for any initial potential value, there exists a distance at which the difference between the observed potential and the one expected in a passive case is maximal. For the degree of nonlinearity in the cockroach giant axon and for depolarizations of 5–20 mV, this distance lies in the range of 0.4–0.6 times the "resting space constant" (Fig. 4*B*). The use of the linear (passive) assumption in this range of distances and potentials results in a 5–30% underestimation of the actual potential decay. For example, in the axon analyzed in Fig. 4, an initial potential of 20 mV decays to 8.6 mV [43.2% of $V(0)$] at the distance of $X = 0.5$ (~1.2 mm). The passive decay would be 60.3% of $V(0)$, ~12 mV, at the same distance. The difference between the nonlinear and the linear case diminishes for either a smaller or a larger range of distances. The conclusion is that the use of a linear model for predicting voltage attenuation in a nonlinear axon is only valid for two points that are either very close or very remote from one another.

Four points concerning this method (Eq. 10) should be noted. First, both the current and voltage electrodes must be placed as close together as possible because an I_0-V relation measured with nonadjacent electrodes will result in an overestimation of the real spatial decay. This is due to the increase in the apparent nonlinearity in the I-V relation with distance, as shown in Fig. 3*C* (see also Noble, 1962).

Second, the "space constant" units by which the anatomical distance is scaled (i.e., x vs. X in Eqs. 8 and 10) are essentially arbitrary. The correct application of the method requires only that the units of electrical length correspond to the factor by which the injected current, I_0, is multiplied (e.g., R_{in} in Eq. 10). Hence, if the distance is scaled in units of $\lambda_V = [r_m(V)/r_i]^{1/2}$, where $r_m(V)$ is the membrane resistance at the potential V, then I_0 must be multiplied by the input slope resistance at that potential. In the analysis of the present study, it was convenient

to normalize the distance in units of the "resting space constant" (i.e., λ_0 at $V = 0$).

Third, although this method of extracting $V(X)$ from the I_0-V relation is strictly applicable only to infinite cables, preliminary study shows that, for rectification characteristics similar to those of the giant axon, the method can also be applied to finite cables, if they are not too short electrically. As a rule of thumb, $V(X)$ can be accurately extracted from an I_0-V relation measured at the midpoint of a finite cable with sealed ends if it is longer than three "resting space constants" (Segev, I., unpublished calculations). This result can be intuitively understood by noting that outward-going rectification increases the effective length of such axons such that, with a larger and larger depolarization, they more closely approximate an infinite cable.

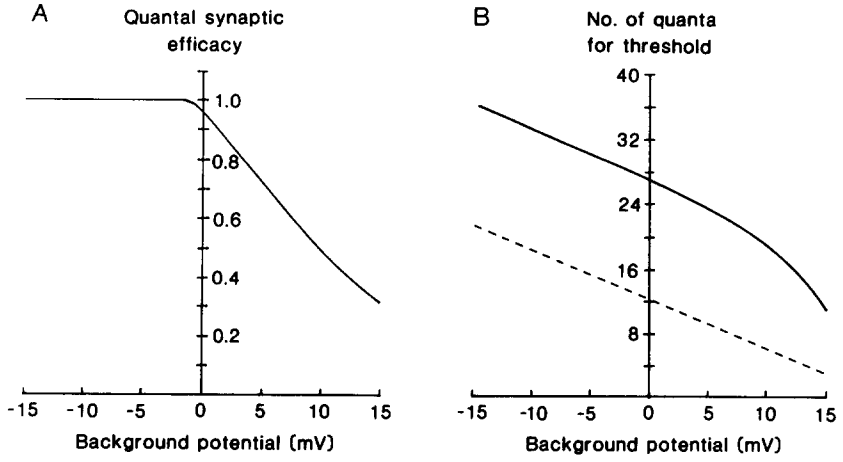

FIGURE 5. Effect of rectification on synaptic efficacy. (*A*) Normalized voltage response to a "quantal" current input of 2 nA injected into the giant axon of Fig. 3*C* as a function of background potential. (*B*) The number of quanta needed to reach threshold for an action potential (20 mV) as a function of background potential (continuous line). The dotted line shows the case of the same axon with passive subthreshold membrane characteristics.

Fourth, it should be noted that the nonlinearity in the experimental I_0-V relation may result from selective contributions of an ionic battery (or batteries) to the measured potential, in addition to the change in the membrane conductance (Grundfest, 1967). The method described in the present study is independent of the ionic mechanisms that are responsible for the nonlinearity. In other words, the spatial attenuation depends on the shape of the I_0-V curve (i.e., on the apparent conductance), and not on its underlying mechanisms.

The results of the present study suggest several functional roles for membrane rectification in neurons at subthreshold potentials. Consider, for example, the effect of rectification near the synaptic site. Tonic changes in background activity, and hence in the apparent "resting potential," will change the input resistance in the region of the synapse, thereby altering its efficacy. This point is illustrated in Fig. 5*A*. A quantal synaptic input is simulated by a constant 2-nA current

pulse injected into the giant axon of Fig. 3*C*. The amplitude of the voltage response, scaled to its maximum, is shown as a function of background potential. The amplitude of this response is reduced by a factor of >3, with a depolarizing background potential of 15 mV (from 1.64 mV at $V = 0$ to 0.53 mV at $V = 15$ mV). The effect of rectification on synaptic efficacy is further demonstrated in Fig. 5*B*. The number of quanta needed to reach threshold for an action potential (20 mV) is shown as a function of background potential for an axon that is linear in the subthreshold voltage range (dotted line) and for the rectifying axon of Fig. 3*C*. At any given background potential below threshold, rectification significantly increases the threshold number of quanta as compared with the passive (linear) case. For example, whereas in the passive case (with zero background potential) only 12 quanta are needed to reach threshold, 27 quanta are needed to discharge the rectifying axon. Rectification of this type may serve as an inhibitory postsynaptic mechanism that reduces the efficacy of synaptic inputs in a nonlinear fashion. Anomalous rectification, of course, will act in the opposite direction.

The effect of rectification on the spatial attenuation of synaptic potentials should also be considered. The method developed here enables a quantitative analysis of this effect. In principle, rectification, combined with changes in the background potential, alters the electrotonic distance between anatomically fixed points, thereby changing the degree of electrical interactions between these points. Hence at some "resting" potentials where the membrane resistivity is high, postsynaptic potentials are large and slow and the electrical length of the dendrites is short. As a result, the degree of interaction between electrical (synaptic) events initiated in different dendrites is enhanced. At other background potentials, where the membrane resistivity is low, postsynaptic potentials are smaller and faster and the dendrites tend to be electrically disconnected. As a result, the dendritic tree could be functionally divided into different compartments with individual dendrites, groups of dendrites, or even portions of one dendrite acting as more or less autonomous units (Segev, I., manuscript in preparation; Kandel and Tauc, 1966).

Thus, the subthreshold nonlinear properties of neuronal membrane can be viewed as a mechanism that allows modulation of the integrative properties of the neuron and contributes to its flexibility in processing information, rather than as a side effect of the membrane excitability.

We are grateful to Dr. J. W. Fleshman for carefully and critically reading this manuscript. We thank Drs. W. Rall, J. Rinzel, and W. Marks for their comments on several early versions of the paper.

This study was supported by the U.S.-Israel Binational Science Foundation grant 2357.

Original version received 6 June 1984 and accepted version received 27 December 1984.

REFERENCES

Adrian, R. H., W. K. Chandler, and A. L. Hodgkin. 1972. An extension of Cole's theorem and its application to muscle. *In* Perspectives in Membrane Biophysics. W. J. Adelman, editor. Gordon and Breach, New York. 299–309.

Anderson, N., and A. M. Arthurus. 1978. Complementary variational principles for steady-state finite cable model of nerve membrane. *Bull. Math. Biol.* 40:735–742.

Arispe, N. J., and J. W. Moore. 1979. Nonlinear cable equations for axons. I. Computations and experiments with internal current injection. *J. Gen. Physiol.* 73:725–735.

Arthurus, A. M., and W. M. Arthurus. 1983. Point bounds for the solution of a nonlinear problem in cell membrane theory. *Bull. Math. Biol.* 45:155–168.

Cole, K. S. 1961. Non-linear current-potential relation in an axon membrane. *J. Gen. Physiol.* 44:1055–1057.

Cole, K. S. 1968. Membranes, Ions and Impulses. University of California Press, Berkeley and Los Angeles, CA. 569 pp.

Cole, K. S., and H. J. Curtis. 1941. Membrane potential of the squid giant axon during current flow. *J. Gen. Physiol.* 24:551–563.

Grundfest, H. 1967. Some comparative biological aspects of membrane permeability control. *Fed. Proc.* 26:1613–1626.

Hodgkin, A. L., and A. F. Huxley. 1952. A quantitative description of membrane current and its application to conduction and excitation in nerve. *J. Physiol. (Lond.).* 117:500–544.

Hodgkin, A. L., and W. A. H. Rushton. 1946. The electrical constants of a crustacean nerve fibre. *Proc. R. Soc. Lond. B Biol. Sci.* 133:444–479.

Jack, J. J. B., D. Noble, and R. W. Tsien. 1975. Electric Current Flow in Excitable Cells. Clarendon Press, Oxford.

Joyner, R. W., and M. Westerfield. 1982. Effect of rectification on synaptic efficacy. *Biophys. J.* 38:39–46.

Kandel, E. R., and L. Tauc. 1966. Anomalous rectification in the metacerebral giant cells and its consequences for synaptic transmission. *J. Physiol. (Lond.).* 183:287–304.

Kerkut, G. A., R. M. Pitman, and R. J. Walker. 1969. Iontophoretic application of acetylcholine and GABA into insect central neurons. *Comp. Biochem. Physiol.* 31:611–633.

Kootsey, J. M. 1977. The steady-state finite cable: numerical method for non-linear membrane. *J. Theor. Biol.* 64:413–420.

Noble, D. 1962. The voltage dependence of the cardiac membrane conductance. *Biophys. J.* 2:381–393.

Rall, W. 1977. Core conductor theory and cable properties of neurons. *In* The Nervous System; Vol. 1: Cellular Biology of Neurons. E. Kandel, editor. American Physiology Society, Bethesda, MD. 39–97.

Redman, S. J. 1976. A quantitative approach to the integrative function of dendrites. *Int. Rev. Physiol.* 10:1–36.

Spira, M. E., I. Parnas, and F. Bergman. 1969. Organization of the giant axons of the cockroach *Periplaneta americana*. *J. Exp. Biol.* 50:615–627.

Spira, M. E., Y. Yarom, and I. Parnas. 1976. Modulation of spike frequency by regions of special axonal geometry and by synaptic inputs. *J. Neurophysiol. (Bethesda).* 39:882–899.

Taylor, R. E. 1963. Cable theory. *In* Physical Techniques in Biological Research. W. L. Natsuk, editor. Academic Press, Inc., New York. 6:219–262.

Trifonov, Yu. A., A. L. Byzov, and L. M. Chailahian. 1974. Electrical properties of subsynaptic and nonsynaptic membranes of horizontal cells in fish retina. *Vision Res.* 14:229–241.

Turner, D. A., and P. A. Schwartzkroin. 1984. Passive electrotonic structure and dendritic properties of hippocampal neurons. *In* Brain Slices. R. Dingledine, editor. Plenum Publishing Corp., New York. 25–50.

Yarom, Y. 1978. Physiological and morphological differentiation of giant axons during the development of the cockroach *Periplaneta americana*. Ph.D. Thesis. Hebrew University, Jerusalem, Israel. 120 pp.